The Molecular g-Tensor, the Magnetic Susceptibility Anisotropy, and the Molecular Electric Quadrupole Moment Tensor of Monofluoroacetonitrile, a Rotational Zeeman Effect Study

H. Krause and D. H. Sutter

Institut für Physikalische Chemie der Universität Kiel, Bundesrepublik Deutschland

Z. Naturforsch. **46a**, 1049–1054 (1991); received October 4, 1991

The rotational Zeeman effect of $H_2F^{12}C^{12}C^{14}N$ was observed at fields up to 20 kG (2 Tesla). The observed vibronic ground state expectation values for the molecular g-values, the magnetic susceptibility anisotropies and the molecular electric quadrupole moments, all referred to the molecular principal inertia axes system, are: $g_{aa} = -0.03572\,(11)$, $g_{bb} = -0.03438\,(7)$, $g_{cc} = -0.03988\,(6)$, $2\,\xi_{aa} - \xi_{bb} - \xi_{cc} = -14.58\,(10) \cdot 10^{-6}$ erg/(G^2 mole), $2\,\xi_{bb} - \xi_{cc} - \xi_{aa} = 1.60\,(11) \cdot 10^{-6}$ erg/(G^2 mole), $Q_{aa} = -9.13\,(6)$ DÅ, $Q_{bb} = 4.17\,(7)$ DÅ, and $Q_{cc} = 4.96\,(9)$ DÅ, respectively. The latter are in close agreement with the results of a restricted Hartree Fock self consistent field calculation with a basis of TZVP quality, which was carried out at the partial r_0-structure determined earlier. Therefore the RHF/TZVP-value for the second electronic moment perpendicular to the heavy atom plane, $\langle 0|\sum c_\varepsilon^2|0\rangle_{\mathrm{RHF}}$, was used as additional input to predict the molecular bulk susceptibility and the individual components of the magnetic susceptibility tensor.

Introduction

In an earlier publication [1] we have presented a partial r_0-structure for monofluoroacetonitrile (for the definition of an r_0-structure see Chapt. XIII in [2]). It was derived from the experimental rotational constants of three isotopomers, $H_2F^{12}C^{12}C^{14}N$ [3], $H_2F^{12}C^{12}C^{15}N$ [4], and $D_2F^{12}C^{12}C^{14}N$ [1], supplemented by our experimental knowledge of the complete ^{14}N nuclear quadrupole coupling tensor. The latter was used as extra information on the bending angle of the CCN chain.

In the following we present the results of a rotational Zeeman effect study of the most abundant isotopomer, $H_2F^{12}C^{12}C^{14}N$. Such a study directly leads to experimental vibronic ground state expectation values for the diagonal elements of the molecular g-tensor and for the anisotropies in the diagonal elements of the molecular magnetic susceptibility tensor. Indirectly, through combinations of these Zeeman parameters, it also leads to experimental values for the diagonal elements of the molecular electric quadrupole moment tensor and for the anisotropies in the second moments of the electronic charge distribution, as described for instance in Chapt. II of the review article on the molecular Zeeman effect by Sutter and Flygare [5].

Reprint requests to Prof. Dr. Dieter H. Sutter, Institut für Physikalische Chemie der Christian-Albrechts-Universität, Olshausenstr. 40–60, W-2300 Kiel, F.R.G.

In the following section we briefly comment on the experimental conditions and on the analysis of the observed Zeeman patterns and we give the derived molecular parameters. In the final section we compare the experimental results to the corresponding values calculated with the restricted Hartree-Fock self consistent field routine from the GAUSSIAN 86 program package [6], and we combine the RHF value for the second moment of the electron distribution perpendicular to the heavy atom plane, $\langle 0|\sum c_\varepsilon^2|0\rangle_{\mathrm{RHF}}$, with our experimental g-values and susceptibility anisotropies to predict the bulk susceptibility as well as the individual components of the magnetic susceptibility tensor.

Experimental Details and Analysis

The sample was prepared as described in [1] by dehydrating monofluoroacetamide powder with phosphorous pentoxide at low pressure. At frequencies below 19 GHz the spectra were recorded with our Stark-effect modulated superheterodyne bridge spectrometer [7]. At higher frequencies, i.e. in the 32 GHz region, J-band absorption cells with an effective length of 180 cm and 8 kHz square wave Stark-effect modulation were used. The spectra were taken at temperatures close to $-50\,^\circ$C and at pressures around 1 mTorr. Typical experimental linewidths were on the order of 70 kHz (full width at half height). In Fig. 1 we

0932-0784 / 91 / 1200-1049 $ 01.30/0. – Please order a reprint rather than making your own copy.

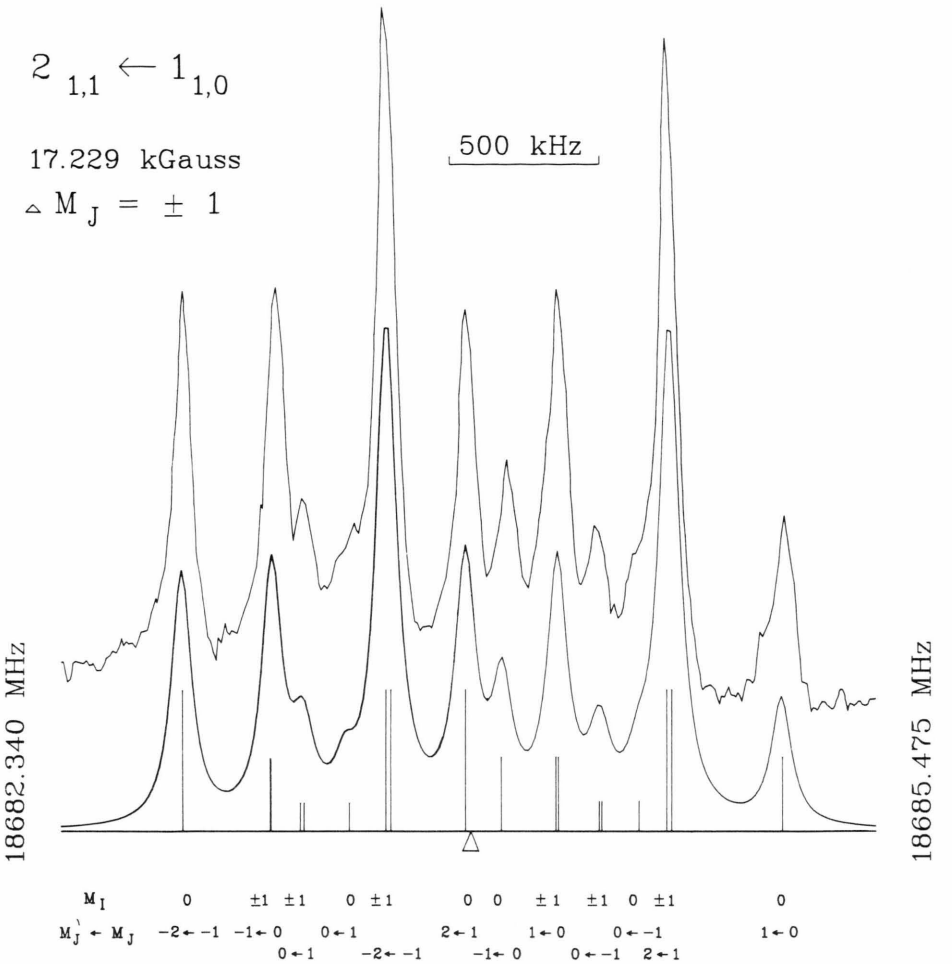

Fig. 1. Recording of the rotational Zeeman effect multiplet corresponding to the $2_{11} \leftarrow 1_{10}$ rotational transition of $H_2F^{12}C^{12}C \equiv {}^{14}N$. It was observed under $|\Delta M_J| = 1$ selection rule in a field of 17.229 kG (1.7229 Tesla). The M-quantum numbers of the limiting uncoupled basis are used to designate the satellites (see text). The simulation (lower trace) was calculated from the optimized g-values and susceptibility anisotropies presented in Table 2 and from the ^{14}N quadrupole coupling constants and rotational constants determined earlier [1]. Lorentzian line shapes with a full width of 80 kHz at half height were assumed for the simulation. The open triangle below the simulation marks the position of the hypothetical center frequency, i.e. the zero field frequency, which would be observed if no quadrupole coupling were present. The satellite frequencies are given in Table 1.

present the Zeeman multiplet of the $2_{11} \leftarrow 1_{10}$ rotational transition observed under $|\Delta M_J| = 1$ selection rule in a field of 17.299 kG. Here M_J measures the component of the rotational angular momentum in the direction of the exterior field. M_I is used as the quantum number for the corresponding component of the ^{14}N nuclear spin. Actually, due to the presence of nitrogen quadrupole coupling and spin rotation coupling, M_J and M_I have lost their meaning as good quantum numbers. We note, however, that the comparatively strong exterior field almost uncouples spin and overall rotation. Thus the uncoupled basis,

$$|J, K_a K_c, M_J\rangle |I, M_I\rangle,$$

where $|J, K_a K_c, M_J\rangle$ is the asymmetric top wavefunction and where $|I, M_I\rangle$ is the wavefunction describing the orientation of the nitrogen spin, comes close to the true eigenfunctions, and our use of the quantum numbers M_J and M_I for state designation is appropriate. In principle, spin rotation coupling, also for the spin-1/2 nuclei F and H, leads to small additional splittings. But since these are well below the resolution of

Table 1. $|\Delta M_J| = 1$-Zeeman multiplet of the $2_{11}-1_{10}$ rotational transition of CH_2FCN in a field of 17.229 kG (compare Fig. 1). The splittings, $\Delta\nu$, are given relative to the hypothetical center frequency of the zero-field ^{14}N quadrupole hyperfine multiplet, 18683.736 MHz. The calculated splittings follow from the optimized Zeeman parameters presented in Table 2 and from the ^{14}N nuclear quadrupole coupling constants and rotational constants given earlier in [1]. All frequencies are in MHz, except for the deviations between the experimental and calculated splittings, Δ, which are in kHz (*.*** = not evaluated because of insufficient signal to noise ratio).

M_I	$M_J - M_J$		rel. int.	$\Delta\nu_{exp}$	$\Delta\nu_{calc.}$	$\Delta\nu_{calc.}$	Δ
−1	−2	−1	120	−0.275	−0.277	−0.285	2
+1	−2	−1	120			−0.269	
0	−2	−1	120	−0.963	−0.963	−0.963	0
−1	0	−1	20	0.406	0.410	0.401	−4
+1	0	−1	20			0.418	
−1	−1	0	60	−0.653	−0.650	−0.647	−3
+1	−1	0	60			−0.652	
0	−1	0	60	0.109	0.107	0.107	2
−1	+1	0	60	0.279	0.286	0.289	−7
+1	+1	0	60			0.283	
0	+1	0	60	1.018	1.016	1.016	2
−1	0	1	20	−0.557	−0.550	−0.556	−7
+1	0	1	20			−0.543	
−1	2	1	120	0.658	0.654	0.647	4
+1	2	1	120			0.661	
0	2	1	120	−0.015	−0.014	−0.014	−1
0	0	−1	20	*.***	0.535	0.535	
0	0	1	20	*.***	−0.411	−0.411	

Table 2. Diagonal elements of the molecular g-tensor and anisotropies in the diagonal elements of the magnetic susceptibility tensor resulting from a least squares fit to a total of 109 Zeeman-satellite frequencies such as shown in Table 1. The rotational constants and ^{14}N nuclear quadrupole constants, which enter into the theoretical expressions for the Zeeman-splittings, were taken from [1]. The indices, a, b, and c, refer to the principal inertia axes.

g_{aa}	−0.03572 (11)
g_{bb}	−0.03438 (7)
g_{cc}	−0.03988 (6)
$2\xi_{aa}-\xi_{bb}-\xi_{cc}$	$-14.58\,(10)\cdot 10^{-6}$ erg/(G^2 mole)
$2\xi_{bb}-\xi_{cc}-\xi_{aa}$	$1.60\,(11)\cdot 10^{-6}$ erg/(G^2 mole)

the spectrometer and leave the intensity weighted means of the satellites unchanged, spin rotation coupling was neglected.

To extract the experimental satellite frequencies from the recorded spectra we have used the methods described in [1] and [8]. The satellite frequencies corresponding to the Zeeman multiplet shown in Fig. 1 are given in Table 1. Within the present investigation we have recorded the Zeeman multiplets of the $1_{01} \leftarrow 0_{00}$, $2_{02} \leftarrow 1_{01}$, $2_{12} \leftarrow 1_{11}$, $2_{11} \leftarrow 1_{10}$, $1_{10} \leftarrow 1_{01}$, and $2_{11} \leftarrow 2_{02}$ rotational transitions at fields up to 20 kG (2 Tesla). A total of 109 satellite frequencies was used to fit the accessible Zeeman parameters, i.e. the three g-values, g_{aa}, g_{bb}, g_{cc}, and the magnetic susceptibility anisotropies, $2\xi_{aa}-\xi_{bb}-\xi_{cc}$ and $2\xi_{bb}-\xi_{cc}-\xi_{aa}$ to the observed shifts of the satellites with respect to the hypothetical center frequencies of the corresponding zero field ^{14}N quadrupole hfs multiplet. The complete frequency listing has been deposited under the reference number TNA 25 at the library of the University of Kiel*. Upon request it may also be obtained from the authors.

The observed Zeeman-hfs-multiplets were analyzed as described in [8], ((6) through (10)), but under neglect of the spin rotation interaction (see above). The ^{14}N nuclear quadrupole coupling constants and the rotational constants, which enter into the theoretical expressions of the Zeeman shifts, were taken from Tables 3 and 6 of [1], respectively. In Table 2 we present our results. Here and throughout this contribution the uncertainties correspond to single standard deviations. As described in Chapt. III, D of [5], the sign of the g-values could be determined unambigously from intermediate field Zeeman multiplets such as the one shown in Figure 2. We note that the indices a, b, and c in Table 2 refer to the principal inertia axes rather than to the principal axes of the g- or the ξ-tensor. For the orientation of the principal inertia axes system with respect to the nuclear frame we refer to Fig. 1 in [1].

The Molecular Electric Quadrupole Moment, the Anisotropies in the Second Moments of the Electronic Charge Distribution, and the So-Called Paramagnetic Susceptibilities

With the rotational constants (Table 6 in [1]) as additional input, the g-values and the susceptibility anisotropies can be used to derive experimental values for the aa-, bb- and cc-component of the molecular electric quadrupole moment tensor (see (14) in [8] and references cited therein). Additional input of the second moments of the nuclear charge distribution, which can be calculated from the partial r_0-structure (see Table 4 in [1]), also allows for the derivation of experimental values for the anisotropies in the second moments of the electronic charge distribution and

* Universitätsbibliothek der Christian-Albrechts-Universität, Westring, W-2300 Kiel, F.R.G.

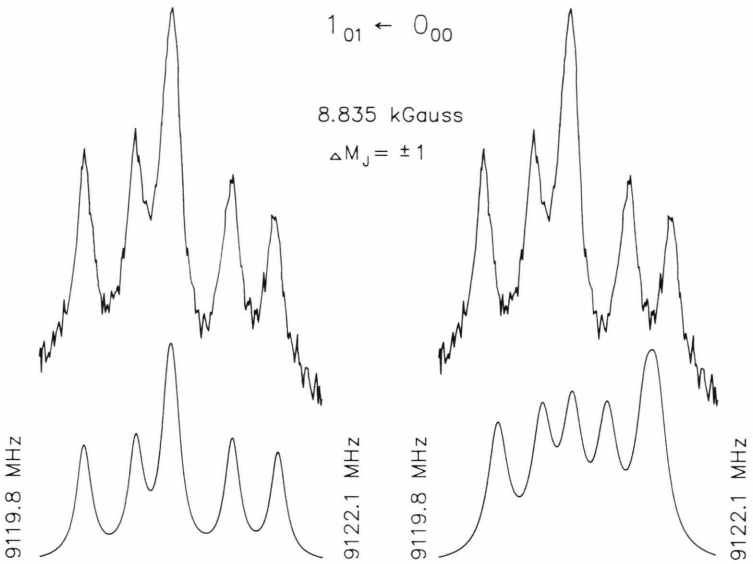

Fig. 2. Two sets of g-values, which only differ in sign, would fit to the high-field spectra (see text). In molecules containing nuclei with a nonzero quadrupole moment, the correct set of g-values can be determined experimentally from intermediate field multiplets such as shown here. The simulation based on positive g-values (at right) clearly differs from the experimental pattern, while the simulation based on negative g-values (at left) nicely fits the observation.

Table 3. Principal inertia axes coordinates of the nuclei in CH_2FCN calculated from the partial r_0-structure presented in [1]. We estimate their uncertainties to be on the order of 0.01 Å.

Nucleus	a/Å	b/Å	c/Å
C	−0.5661	−0.6294	0.000
F	−1.4700	0.4183	0.000
H	−0.7341	−1.2463	0.8795
H	−0.7341	−1.2463	−0.8795
C	0.8010	−0.1169	0.0000
N	1.8988	0.2514	0.0000

Table 4. The molecular electric quadrupole moments, the anisotropies in the second moments of the electron coordinates, and the so-called paramagnetic susceptibilities as they follow from the experimental g-values, the experimental susceptibility anisotropies and the nuclear coordinates of the partial r_0-structure given in Table 3. At the right hand side we give the corresponding RHF/6-311 G** values for comparison. They too were calculated at the nuclear configuration presented in Table 3.

	exp.	RHF/6-311 G**
Q_{aa}	−9.130 (62) DÅ	−9.6383 DÅ
Q_{bb}	+4.173 (74) DÅ	+5.1195 DÅ
Q_{cc}	+4.957 (92) DÅ	+4.5188 DÅ
$\langle 0\vert\sum(a_e^2-b_e^2)\vert 0\rangle$	45.81 (53) Å^2	46.0049 Å^2
$\langle 0\vert\sum(b_e^2-c_e^2)\vert 0\rangle$	6.14 (8) Å^2	5.9518 Å^2
$\langle 0\vert\sum(c_e^2-a_e^2)\vert 0\rangle$	−51.95 (52) Å^2	−51.9567 Å^2
χ^p_{aa}	40.81 (33) · 10^{-6} erg/(G^2 mole)	
χ^p_{bb}	240.54 (221) · 10^{-6} erg/(G^2 mole)	
χ^p_{cc}	270.38 (223) · 10^{-6} erg/(G^2 mole)	

for the so-called paramagnetic susceptibilities (see (16) in [8] and (I.4) in [5], resp.). In Table 3 we give the corresponding principal inertia axes coordinates of the nuclei. From them and from the atomic numbers, Z_n, the second nuclear moments follows as $\sum Z_n a_n^2 = 51.54\,(52)$ Å^2, $\sum Z_n b_n^2 = 7.58\,(8)$ Å^2, and $\sum Z_n c_n^2 = 1.55\,(2)$ Å^2, where the summation index, n, runs over the nuclei. A 1% uncertainty was assumed for these values in order to account for the fact that only a partial r_0-structure is available. We present our derived molecular parameters on the left hand side in Table 4. The uncertainties represent single standard deviations in units of the least significant digit, as they follow by Gaussian error propagation from the experimental data. We note that the uncertainties for the anisotropies in the second electronic moments and those for the paramagnetic susceptibilities are largely determined by the 1% uncertainties assumed for the nuclear second moments. Thus they could be reduced considerably if a further improved molecular structure were available.

Comparison to Quantum Chemical Results and Prediction of the Bulk Susceptibility and the Individual Components of the Molecular Susceptibility Tensor

For comparison we have also carried out quantum chemical calculations. To this end we did run the re-

Table 5. Magnetic susceptibilities and second moments of the electronic charge distribution derived from the experimental g-values, susceptibility anisotropies, rotational constants, and nuclear coordinates, under additional input of the RHF/6-311 G**-value for the second electronic moment perpendicular to the heavy atom plane, $\langle 0|\sum c_e^2|0\rangle_{RHF}$. In brackets we also give the RHF-values for the other two second electronic moments for comparison.

ξ_{aa}	$-35.59\,(85)\cdot 10^{-6}$ erg/(G^2 mole)
ξ_{bb}	$-30.16\,(85)\cdot 10^{-6}$ erg/(G^2 mole)
ξ_{cc}	$-26.36\,(85)\cdot 10^{-6}$ erg/(G^2 mole)
ξ_{bulk}	$-30.69\,(85)\cdot 10^{-6}$ erg/(G^2 mole)
$\langle 0\|\sum a_e^2\|0\rangle_{semi\,exp.}$	57.98 (53) Å^2
$(\langle 0\|\sum a_e^2\|0\rangle_{RHF})$	(57.886 Å^2)
$\langle 0\|\sum b_e^2\|0\rangle_{semi\,exp.}$	12.07 (12) Å^2
$(\langle 0\|\sum b_e^2\|0\rangle_{RHF})$	(11.882 Å^2)
$\langle 0\|\sum c_e^2\|0\rangle_{RHF}$	5.930 Å^2

Table 6. Comparison between the experimental [1] and the RHF-values for the ^{14}N nuclear quadrupole coupling constants in $H_2F^{12}C^{12}C^{14}N$. For the conversion from the RHF-values for the electric field gradients at N to the coupling constants the factor 4.001596 MHz/a.u. was used (see text). The RHF-values were calculated at the partial r_0-structure presented in Table 3.

	exp.	RHF/6-311 G**
χ_{aa}/MHz	−3.7039 (26)	−3.68948
χ_{bb}/MHz	+1.8918 (26)	+1.96610
χ_{cc}/MHz	+1.8122 (37)	+1.72867
χ_{ab}/MHz	−2.119	−2.17531

stricted Hartree-Fock self consistent field routine from the GAUSSIAN 86 program package, mounted at the CRAY X-MP 216 machine of the computer center at the University of Kiel. The calculation was carried out for our partial r_0-structure given in Table 3. We have used the triple zeta valence basis plus polarization functions (TZVP-basis), i.e. the 6-311 G** basis, which includes additional p-functions at H and d-functions at C, N, and F. Inclusion of polarization functions leads to a better prediction of the molecular electric quadrupole moment tensor, while in certain cases it may slightly worsen the prediction for the electric field gradients at the positions of the nuclei [9]. The latter, however, was not found in the present study. We present the results on the right hand side in Table 4. In view of the fair agreement between the experimental and the RHF/6-311 G** results for the molecular electric quadrupole moment, we ventured to use the RHF-value for the second electronic moment perpendicular to the heavy atom plane, $\langle 0|\sum c_e^2|0\rangle$, as additional input for a prediction of the values for the bulk susceptibility and for the individual components of the magnetic susceptibility tensor from our g-values and susceptibility anisotropies (see (17) in [8]). The results are given in Table 5. Furthermore, since the anisotropies in the second electronic moments are known from the experiment (see Table 4), the additional input of the 6-311 G** value $\langle 0|\sum c_e^2|0\rangle$ also leads to "semi experimental" values for the remaining two second electronic moments, and so we present them too in Table 5 for comparison with their RHF counterparts.

Finally, in Table 6, we compare the experimental ^{14}N nuclear quadrupole coupling constants [1] with the corresponding electric field gradients at the ^{14}N nucleus as calculated with the RHF routine. For the conversion from the field gradients to the experimentally accessible quadrupole coupling constants we have used the factor 4.001596 MHz/a.u. This value has been obtained from a least squares fit between the experimental quadrupole coupling constants and the corresponding 6-311 G** field gradients of a larger set of nitriles [10]. It would correspond to a ^{14}N nuclear quadrupole moment of only $17.03\,(10)\cdot 10^{-27}$ cm^2 as compared to the currently accepted value of $19.9\,(2)\cdot 10^{-27}$ cm^2 [11]. As was discussed for instance in [9], the use of such an effective conversion factor at least partly accounts for the limited precission in the electronic wavefunction. It is basis set and method dependent (i.e. SCF versus C.I. etc.). For ^{14}N it also depends on the local environment of the nitrogen nucleus within the molecule. For instance for a set of imines an even smaller conversion factor, corresponding to a nuclear quadrupole moment of only $16.84\cdot 10^{-27}$ cm^2 has been found for the best prediction of the quadrupole couplings from the RHF/6-311 G** electric field gradients [12].

Acknowledgements

We gratefully acknowledge the support by Deutsche Forschungsgemeinschaft and Fonds der Chemie. The quantum chemical calculations were performed at the computer center of the University of Kiel.

[1] M. Andolfatto, H. Krause, D. H. Sutter, and M. H. Palmer, Z. Naturforsch. **43a,** 651 (1988).
[2] Walter Gordy and Robert L. Cook, Microwave Molecular Spectra, 2nd Edition (1984), John Wiley, New York.
[3] W. Kasten, H. Dreizler, B. E. Job, and J. Sheridan, Z. Naturforsch. **38a,** 1015 (1983).
[4] H. Zerbe and A. Guarnieri, Z. Naturforsch. **42a,** 1275 (1987).
[5] D. H. Sutter and W. H. Flygare, Topics in Current Chem. **63,** 91 (1976).
[6] M. J. Frisch, M. Head-Gordon, H. B. Schlegel, K. Raghavachari, J. S. Binkley, C. Gonzales, D. J. Defrees, D. J. Fox, R. A. Westside, R. Seeger, C. F. Melius, J. Baker, R. L. Martin, L. R. Kahn, J. J. P. Stewart, E. M. Fluder, S. Topiol, and J. A. Pople, Gaussian Inc., Pittsburgh.
[7] W. H. Stolze, M. Stolze, D. Hübner, and D. H. Sutter, Z. Naturforsch. **37a,** 1165 (1982).
[8] H. Krause, D. H. Sutter, and M. H. Palmer, Z. Naturforsch. **44a,** 1063 (1989).
[9] J. Spieckermann and D. H. Sutter, Z. Naturforsch. **46a,** 715 (1991).
[10] H. Krause, private communication (manuscript in preparation for publication in Z. Naturforsch.).
[11] P. Pyykkö, Proc. 11th ISNQR, to be published in Z. Naturforsch. **47a** (1992).
[12] H. Krause and D. H. Sutter, Z. Naturforsch. **46a** (1991), in press.